Chemical Structure and Superconductivity

R. B. King

Department of Chemistry, University of Georgia, Athens, Georgia 30602

Received April 15, 1998

Consideration of the chemical bonding topology of the conducting skeletons in the Chevrel phases MMo_6S_8 and the lanthanide rhodium borides $LnRh_4B_4$ indicates that the conducting skeletons consist of networks of edge-localized bonded atoms. These observations suggest that superconductivity is favored when electron mobility is restricted to fewer than three dimensions. Thus, the chemical bonding topologies of the highest T_c superconductors contain one of the following features: (1) edge-localized M−M bonding in the conducting skeletons of ternary and quaternary solid-state superconductors or related, partially localized bonding in superconducting transition metals and their alloys; (2) localized rather than fully delocalized bonding in copper oxide superconductors containing Cu−O−Cu linkages with appreciable Cu···Cu antiferromagnetic interactions; or (3) surface-localized bonding in fullerene superconductors containing direct C−C bonds such as K_3C_{60}. In addition, heavy fermion superconductors with considerably lower T_cs values are known in which the conducting skeleton consists of variable oxidation state lanthanide or actinide cations diluted by an anionic network of other metal atoms so that the lanthanide or actinide atoms are not within bonding distance of each other.

1. INTRODUCTION

In recent years there has been increasing interest in developing structure−activity relationships based on molecular topology. The greatest focus has been on the use of so-called topological indices as chemical behavior descriptors.[1,2] Such topological indices in the classical sense describe the connectivity of a molecular network and do not necessarily pertain to the details of chemical bonding. Furthermore, most work in molecular topology has been limited to organic structures containing mainly first-row atoms without chemically accessible d-orbitals. The chemical bonding in such structures is thus largely limited to four-orbital sp^3 manifolds without any multicenter bonding.

A question of interest to the author for approximately a quarter century has been the extension of topological concepts to problems in inorganic chemistry. In such cases the diversity of chemical bonding is much more extensive than in organic chemistry and includes chemically active d-orbitals in transition metals leading to many six-coordinate octahedral structures with sp^3d^2 hybridization and even considerably more complicated coordination polyhedra derivable from nine-orbital sp^3d^5 manifolds. A variety of cage and cluster structures with multicenter bonding also frequently arise in inorganic chemistry including, for example, a variety of cage borane structures based on deltahedra as well as diverse transition metal clusters and metal−metal multiple bonding. Many of the author's efforts in developing applications of topology in inorganic chemistry are summarized in a review article several years ago[3] and a subsequent book.[4]

After the author had developed a number of topological approaches for understanding many aspects of structural inorganic chemistry, it next became of interest to use related methods for developing structure−property relationships in inorganic compounds. The property of interest was superconductivity;[5−8] namely, the ability to conduct electricity without resistance below a certain critical temperature, typically denoted by T_c. At the time that this work was initiated in 1985, the highest known T_cs were only ∼20 K, which considerably limited the practical applications of superconductors. The author initiated his study with a consideration of the so-called Chevrel phases; namely, ternary molybdenum chalcogenides of the general formula $M_nMo_6S_8$ and $M_nMo_6Se_8$, containing chemically bonded Mo_6 octahedra that have T_cs approaching 15 K for $PbMo_6S_8$ in addition to having relatively high critical fields.[9] At that time, the author also considered the structures of the ternary lanthanide rhodium borides of the type $LnRh_4B_4$ (Ln = Nd, Sm, Er, Tm, Lu, etc.) containing chemically bonded Rh_4 tetrahedra similar to the Rh_4 tetrahedron in the molecular carbonyl $Rh_4(CO)_{12}$, and which had the highest known T_c at the time for any type of solid-state boride (e.g., for $LuRh_4B_4$, $T_c = 11.5$ K[10]). Consideration of these two types of ternary solid-state structures, which are diverse except for the presence of polyhedra with metal−metal bonding localized along the polyhedral edges, led to the observation that superconductivity is favored (i.e., the T_c is maximized) when electron mobility is restricted to fewer than three dimensions (i.e., the corresponding conducting subnetwork is a porous structure with edge-localized rather than highly delocalized bonding). Traditional physical theories of superconductivity, notably the Nobel-Prize-winning theory of Bardeen, Cooper, and Schrieffer,[11] have led to a useful phenomenological understanding of superconductivity but do not provide clear correlations between superconductivity and molecular structure.

The field of superconductivity was revolutionized almost immediately after the publication of the author's original two papers on the chemical bonding topology of superconductors[9,10] when the first high T_c superconducting copper oxides

10.1021/ci980050b CCC: $18.00
Published on Web 08/20/1998

were discovered.[12−14] Subsequent development of the chemistry of high T_c superconducting copper oxides led to superconductors with T_cs as high as 130 K, a considerable improvement of the maximum T_c of only ~20 K in the days before copper oxides. Shortly after the recognition of certain copper oxide structures as high T_c superconductors, the author showed how the idea of a porous conducting subnetwork, developed by consideration of the Chevrel phases[9] and the ternary rhodium borides,[10] could be extended to the copper oxides.[15]

Subsequent work by the author since 1988 has extended the topological treatment of the chemical bonding in superconductors to other important types of superconductors such as other ternary solid-state silicides and borides, the A-15 alloy superconductors M_3E (M = V, Nb, Ta; E = Si, Ge, Sn), and transition metal alloys in 1990;[16] the layered quaternary lanthanide nickel borocarbides and boronitrides in 1996;[17] and, most recently, the heavy fermion superconductors in 1997.[18] The author has reviewed his work on the chemical topology of superconductors most recently in 1996.[19] This articles focuses on examples of the structure−property relationships found in inorganic superconductors with particular focus on new insight obtained by the recent consideration of the heavy fermion superconductors.[18] The reader is referred to the earlier articles for chemical and structural details beyond the scope of the present article.

2. CONDUCTING SKELETONS OF SUPERCONDUCTING MATERIALS

Treatments of the chemical bonding topologies of ternary and quaternary solid-state materials, including those with superconducting properties, first partition their structures into positive ions of the alkali, alkaline earth, lanthanide, or actinide metal present in the structure and a negative charged network containing the remaining elements. The nature of this anionic subnetwork determines the electrical properties of the structure as follows:

(1) Conductivity arises either from holes in the valence band [i.e., the highest occupied molecular orbital (HOMO)] leading to *p*-type conductors or from electrons in the conduction band [i.e., the lowest unoccupied molecular orbital (LUMO)] leading to *n*-type conductors. An anionic subskeleton of either type may be described as a conducting skeleton.

(2) Superconductivity arises when the electron or hole mobility in the conducting skeleton is restricted to fewer than three dimensions; that is, when the electrons or holes leading to conductivity are not free to move throughout the entire three-dimensional space of the conducting skeleton but instead are confined to the edges of the conducting skeleton with a regular pattern of cavities within the conducting skeleton not accessible to the mobile electrons or holes.

The cavities inaccessible to the mobile electrons or holes make the conducting skeleton porous, and the author has called such conducting skeletons porously delocalized.[9,10,19] In chemical terms, a porously delocalized conducting skeleton corresponds to one in which the chemical bonding is most effectively described by two-electron, two-center, edge-localized bonds or other similarly localized bonds within the conducting skeleton. Thus, the identification of superconducting structures consists of finding structures in which the chemical bonding in the conducting skeleton is localized along the edges of the skeleton rather than delocalized throughout the entire volume of the conducting skeleton. In other words, a porous chemical bonding topology involves only the 1-skeleton[20] of the polyhedron in contrast to the dense bonding in a polyhedron that involves the whole volume of the polyhedron.

The electropositive metals forming the positive counterions in the ternary and quaternary solid-state structures normally exhibit a single accessible oxidation state, namely +1 for the alkali metals, +2 for the alkaline earth metals, +3 for most lanthanides, and +4 for thorium. Such positive counterions cannot participate in electron or hole transport and thus are not part of the conducting skeleton. However, a few superconducting structures are known where the electropositive metals are multiple-oxidation-state lanthanides or actinides so that these cations can participate in electron or hole transport. Because the electrons involved in such structures are necessarily f-electrons, superconductors of this type are called heavy fermion superconductors.[21] The sets of f-block metal oxidation states involved in heavy fermion superconductors include particularly Ce(III) ↔ Ce(IV) and U(III) ↔ U(IV) ↔ U(V) ↔ U(VI). An important role in the anionic subnetwork of heavy fermion superconductors is dilution of the cationic subnetwork so that the separation of the f-block metal cations in the structure is at least 4 Å. The T_cs of heavy fermion superconductors are significantly lower than those of other types of superconductors, with the highest known T_c in a heavy fermion superconductor[21] being only ~1.5 K in URu_2Si_2 and U_2PtC_2.

3. TERNARY SOLID-STATE SUPERCONDUCTOR STRUCTURES CONTAINING DISCRETE METAL CLUSTER POLYHEDRA

The correlation of superconducting properties with edge-localized bonding in the conducting skeleton was first developed in structures containing well-defined polyhedral metal cluster units in their conducting skeletons because comparison of these structures with those of well-established discrete molecular species facilitated analysis of the chemical bonding topology. Thus, the author's initial work[9] published in 1987 treated the Chevrel phases, which contain Mo_6 octahedra analogous to those found in the long-known molybdenum(II) halides.[22] This work was immediately followed by a similar treatment of the ternary lanthanide rhodium borides,[10] which contain Rh_4 tetrahedra analogous to that found in $Rh_4(CO)_{12}$.

3.1. Superconductors Containing Metal Cluster Octahedra. The ternary molybdenum chalcogenides of general formula $M_nMo_6S_8$ and $M_nMo_6Se_8$ (M = Ba, Sn, Pb, Ag, lanthanides, Fe, Co, Ni, etc.), commonly known as Chevrel phases,[23,24] were the first superconducting ternary structures found to have relatively high T_cs, reaching 15 K for $PbMo_6S_8$,[25] in addition to having relatively high critical fields. From the structural point of view the Chevrel phases are constructed from Mo_6 octahedra, which may be considered to have a bonding topology analogous to that in the molybdenum(II) halides $Mo_6X_8L_6^{4+}$ (L = two-electron donor ligand).[22] The basic building blocks of the Chevrel phases

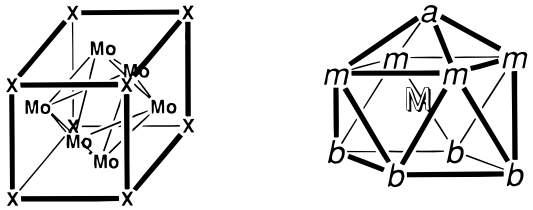

Figure 1. (a) An Mo_6 octahedron within an X_8 cube. (b) The capped square antiprism molybdenum (M) coordination in Mo_6X_8 clusters.

are Mo_6S_8 (or Mo_6Se_8) units containing a bonded Mo_6 octahedron (Mo−Mo distances in the range 2.67 to 2.78 Å) with a sulfur atom capping each face, leading to an Mo_6 octahedron within an S_8 cube (Figure 1a: X = S). Each (neutral) sulfur atom of the S_8 cube functions as a donor of four skeletal electrons to the Mo_6 octahedron within that S_8 cube, leaving a sulfur electron pair to function as a ligand to a molybdenum atom in an adjacent Mo_6 octahedron. Maximizing this sulfur electron pair donation to the appropriate Mo_6 octahedron results in a tilting of the Mo_6 octahedron by ∼25° within the cubic array of the other metal atoms M.[26] These other metal atoms M furnish electrons to these Mo_6S_8 units, allowing them to approach but not attain the $Mo_6S_8^{4-}$ closed-shell electronic configuration. This corresponds to the partially filled valence band of a *p*-type conductor. Electronic bridges between individual Mo_6 octahedra are provided by interoctahedral Mo−Mo interactions, with the nearest *inter*octahedral Mo−Mo distances occurring in the range 3.08−3.49 Å for Mo_6S_8 and Mo_6Se_8 derivatives. The coordination polyhedron of each of the Mo atoms may be described as a capped square antiprism (Figure 1b) with the external ligand (i.e., a sulfur lone pair) in the axial position (*a* in Figure 1b), four bonds to face-bridging sulfur atoms in the four medial positions (*m* in Figure 1b), and the four internal orbitals in the basal positions (*b* in Figure 1b) forming two-center bonds to adjacent Mo atoms.

The fundamental Chevrel phase building block is the closed-shell $Mo_6S_8^{4-}$ unit with the following electron counting scheme, remembering that each molybdenum vertex receives an electron pair from a sulfur atom of an adjacent Mo_6S_8 unit and thus may be treated as an LMo vertex:

6 LMo vertexes: (6)(−2) =	−12 electrons
8 μ_3-S bridges: (8)(4) =	32 electrons
−4 charge:	4 electrons
Total skeletal electrons:	*24 electrons*

These 24 skeletal electrons are the exact number required for an edge-localized octahedron with two-electron, two-center bonds along each of its 12 edges.

This chemical bonding topology of the Chevrel phases MMo_6S_8 consisting of edge-localized discrete Mo_6 octahedra linked through sulfur atoms as well as interoctahedral metal−metal interactions led naturally to the concept of *porous delocalization*.[9] The concept of porous delocalization can be related to the suggestion[27] that the high critical fields of the Chevrel phases MMo_6S_8 arises from a certain localization of the conduction−electron wave function of the Mo_6 clusters, leading to an extremely short mean free path and/or a low Fermi velocity corresponding to a small coherence length in the Bardeen/Cooper/Schrieffer theory already mentioned.

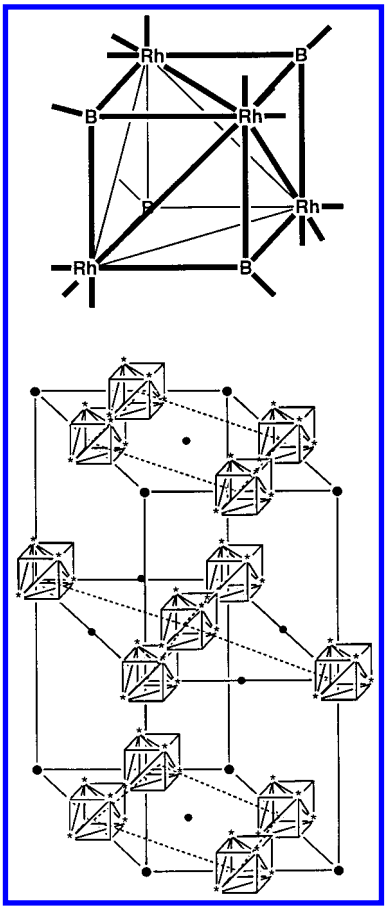

Figure 2. (a) The cube with six diagonals in $LnRh_4B_4$, which is topologically equivalent to a tetracapped tetrahedron. (b) The primitive tetragonal structure of $LnRh_4B_4$ with the cubes, not drawn to scale, representing the Rh_4B_4 units with the Rh vertexes starred.

3.2. Superconductors Containing Metal Cluster Tetrahedra. The ternary lanthanide rhodium borides, $LnRh_4B_4$ (Ln = certain lanthanides such as Nd, Sm, Er, Tm, Lu), are a class of relatively high-temperature non-oxide superconductors[28,29] exhibiting significantly higher T_cs than other types of ternary metal borides (e.g., T_c = 11.5 K for $LuRh_4B_4$). These rhodium borides exhibit structures containing electronically linked discrete Rh_4 tetrahedra. The topology of an individual Rh_4B_4 unit in these ternary borides is that of a tetracapped tetrahedron of T_d symmetry in which the four degree 6 vertices correspond to rhodium atoms and the four degree 3 vertices correspond to boron atoms (Figure 2a). Such a tetracapped tetrahedron is topologically equivalent to a cube with six diagonals drawn to preserve T_d overall symmetry. The diagonals of the Rh_4B_4 cube in the $LnRh_4B_4$ borides correspond to six Rh−Rh bonds (average length 2.71 Å in YRh_4B_4) and the edges of the cube correspond to 12 Rh−B bonds (average length, 2.17 Å in YRh_4B_4).[30] The ratio between these two lengths, namely 2.71/2.17 = 1.25, is only ∼13% less than the $\sqrt{2}$ = 1.414 ratio of these lengths in an ideal cube, suggesting that the Rh_4B_4 building blocks can be approximated by a cube in the three-dimensional lattice. The Rh−Rh distances of 2.71 Å in these Rh_4B_4 units are essentially identical to the mean Rh−Rh distance in the discrete molecular tetrahedral rhodium cluster[31] $Rh_4(CO)_{12}$ that is regarded as a prototypical example of an edge-localized tetrahedron.

The arrangement of the Rh_4B_4 units as sheets in the primitive tetragonal lattice of $LnRh_4B_4$ is shown in Figure 2b. All of the valence orbitals of both the boron and rhodium atoms are involved in the formation of four and nine two-center bonds corresponding to spherical sp^3 and sp^3d^5 manifolds, respectively. The four bonds formed by a boron atom using its sp^3 bonding orbital manifold are as follows:

(1) three bonds to rhodium atoms in the same Rh_4B_4 cube (average Rh−B distance, 2.17 Å in YRh_4B_4);

(2) one bond to the nearest boron atom in an adjacent Rh_4B_4 cube (B−B distance, 1.86 Å in YRh_4B_4), thereby leading to discrete B_2 units in the structure.

The nine bonds formed by a rhodium atom using its sp^3d^5 bonding orbital manifold are as follows:

(1) three bonds to rhodium atoms in the same Rh_4 tetrahedron (average Rh−Rh distance, 2.71 Å in YRh_4B_4);

(2) three bonds to boron atoms in the same Rh_4B_4 cube (average Rh−B distance, 2.17 Å in YRh_4B_4);

(3) one bond to the nearest rhodium atom in another Rh_4B_4 cube in the same sheet (Rh−Rh distance, 2.68 Å in YRh_4B_4);

(4) two bonds to the next-nearest rhodium atoms in adjacent Rh_4B_4 cubes (Rh−Rh distances, 3.14 Å in YRh_4B_4).

In deriving the chemical bonding topology, each boron atom is considered to have three internal orbitals and one external orbital and is therefore a donor of two skeletal electrons because one of the three boron valence electrons is needed for the B−B bond using its external orbital. Similarly, each rhodium atom has six internal orbitals and three external orbitals and is therefore a donor of six skeletal electrons because three of the nine rhodium valence electrons are needed for the three external Rh−Rh bonds formed by a given rhodium atom.

These considerations suggest that a neutral Rh_4B_4 unit in the $LnRh_4B_4$ borides has 32 skeletal electrons as follows:

4 Rh vertexes: (4)(6) =	24 electrons
4 B vertexes: (4)(2) =	8 electrons
total skeletal electrons for each Rh_4B_4 unit:	*32 electrons*

Because a tetracapped tetrahedron or the topologically equivalent cube with six diagonals (Figure 2a) has 18 edges corresponding to six Rh−Rh bonds and 12 Rh−B bonds as just outlined, a closed-shell edge-localized Rh_4B_4 unit requires (2)(18) = 36 skeletal electrons corresponding to the tetraanion $Rh_4B_4^{4-}$. Because the lanthanides also present in the lattice form tripositive rather than tetrapositive ions, the $LnRh_4B_4$ borides must be $Ln^{3+}Rh_4B_4^{3-}$, with the $Rh_4B_4^{3-}$ anion having one electron less than the closed shell electronic configuration $Rh_4B_4^{4-}$. This situation is similar to that already discussed for the Chevrel phases in which, for example, $PbMo_6S_8$ has $Mo_6S_8^{2-}$ units with two electrons less than the closed-shell electronic configuration $Mo_6S_8^{4-}$.

4. OTHER TERNARY AND QUATERNARY SOLID STATE SUPERCONDUCTOR STRUCTURES

4.1. Other Ternary Metal Boride Superconductors. Similar methods can be applied for the analysis of the chemical bonding topology in other ternary metal boride superconductors including derivatives of the types $Ba_{0.67}Pt_3B_2$, $LnRuB_2$, and $LnOs_3B_2$ (Ln = lanthanide).[16] The ternary metal borides exhibiting the next higher T_c to $LnRh_4B_4$ are the borides of the type $LnRuB_2$ (Ln = lanthanide) among which $LuRuB_2$ exhibits a T_c of 10.0 K. The conducting skeletons of $LnRuB_2$ consist of chains of bonded ruthenium atoms (Ru−Ru = 3.03 Å in $LuRuB_2$) in which each ruthenium atom is also bonded to six boron atoms and each boron atom is bonded to three ruthenium atoms leading to $RuB_{6/3}^{4-}$ structural units.[32] The boron atoms are tightly bonded in pairs (B−B = 1.74 Å in $LuRuB_2$ as compared with B−B = 1.86 Å in $LnRh_4B_4$ already discussed) so that each boron atom has two of its three valence electrons available for bonding to ruthenium. The ruthenium atom in such a $RuB_2^{4-} = RuB_{6/3}^{4-}$ structural unit has the following favored 18-electron rare gas configuration:

neutral Ru Atoms	8 electrons
2 Ru−Ru bonds to adjacent Ru atoms in the Ru_n chain	2 electrons
6/3 boron atoms of bonded B_2 pairs as ligands: (6/3)(2) =	4 electrons
−4 charge	4 electrons
electronic configuration of Ru atom in RuB_2^{4-}	*18 electrons*

Because the lanthanides in $LnRuB_2$, like those in $LnRh_4B_4$ already discussed, form tripositive rather than tetrapositive ions, the ruthenium atoms in $LnRuB_2$ have one valence electron less than the 18-electron closed-shell electronic configuration of RuB_2^{4-}. This electron deficiency corresponds to the presence of holes in an otherwise filled valence band, thereby providing a mechanism for conductivity. Furthermore, the conducting skeleton of $LnRuB_2$ consists solely of two-electron two-center B−B, Ru−B, and Ru−Ru bonds, leading to the edge-localized type of conducting skeleton associated with superconductivity.

4.2. The Quaternary Metal Boride Carbides LnM_2B_2C (M = Ni, Pd, Pt). Quaternary metal boride carbides of the type LnM_2B_2C (M = Ni, Pd, Pt) in favorable cases were recently[33] found to exhibit higher superconducting T_cs than any of the ternary metal borides including the $LnRh_4B_4$ and $LnRuB_2$ derivatives already discussed. Thus, the T_c of $LuNi_2B_2C$ was 16.6 K.[34]

The general structures of the LnM_2B_2C superconductors as well as the related nonsuperconducting materials of the type LnNiBC are depicted schematically in Figure 3. These structures consist of square nets of nickel atoms with boron atoms above and below the nickel nets. In the LnM_2B_2C superconductors, the nickel nets are linked by net-bridging linear $[:B{=}C{=}B:]^{2-}$ ligands that because of the short B=C distances (1.47 Å) and linear two-coordinate carbon atom can be considered to have boron−carbon multiple bonds with an sp-hybridized central carbon atom. The boron atoms of such BCB ligands can also be regarded as sp-hybridized with an electron pair in an sp hybrid on each boron atom pointing away from the central carbon atom as well as an empty p orbital similar to the empty p orbital in simple boron trihalides BX_3 (X = F, Cl, Br, I). In the Ni_2B_2C conducting skeletons of $LnNi_2B_2C$ derivatives, the electron deficiency of this empty p orbital on each boron atom of the BCB ligands is relieved by forming a multicenter bond with the nickel atoms in the nickel square net. In addition, another multicenter bond is formed between the boron sp-hybrid orbital and a pair of nickel atoms. Each BCB ligand is linked to a total of eight nickel atoms through such multicenter bonding and any given nickel atom is linked to four boron atoms in an approximately tetrahedral arrangement leading to $Ni(BCB)_{4/8}$ as a descriptor of the ligands around a single nickel atom. Halet[33] uses the oxidation state formalism

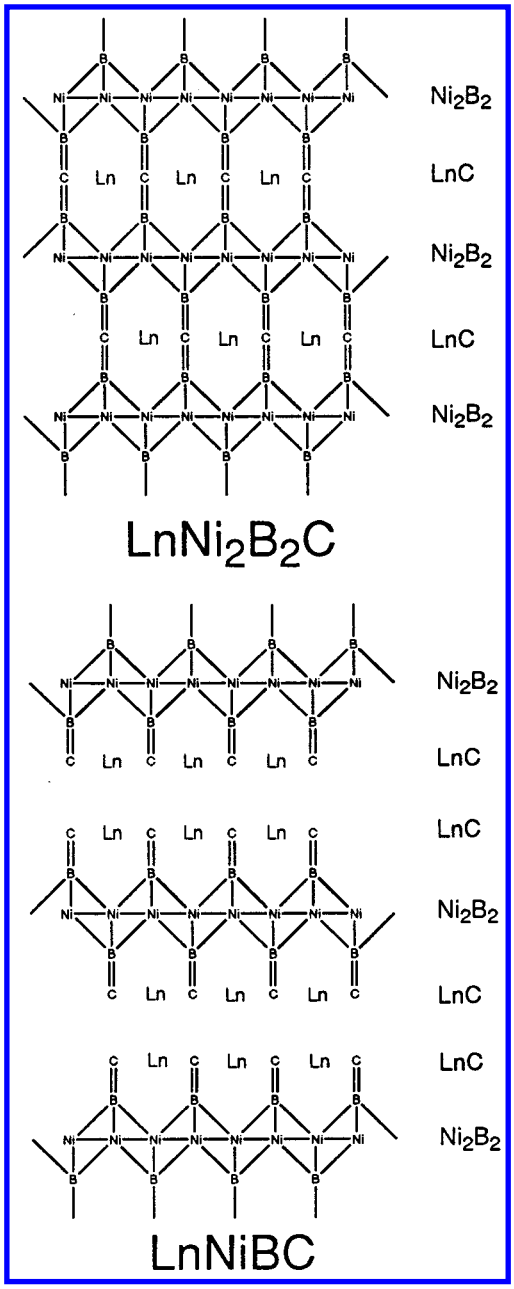

Figure 3. (a) Schematic representation of the layer structure of the $LnNi_2B_2C$ superconductors. (b) Schematic representation of the layer structure of LnNiBC.

$(Ln^{2+})(Ni^0)_2(B_2C)^{2-}$ to describe $LnNi_2B_2C$ and notes the resemblance of the tetrahedral Ni^0B_4 unit in $LnNi_2B_2C$ to the tetrahedral Ni^0C_4 unit in $Ni(CO)_4$. However, the direct bonding of a given nickel atom to four other nickel atoms in $LnNi_2B_2C$ as contrasted with the absence of Ni−Ni bonds in $Ni(CO)_4$ suggests that this resemblance is fortuitous.

Elementary electron counting suggests that $Ni(B_2C)_{4/8}^{3-}$ is a closed shell configuration.[17] Thus, the actual formula $LnNi_2B_2C$ corresponding to $Ni(B_2C)_{4/8}^{1.5-}$ is deficient by 1.5 electrons per nickel atom although the partial multiple bonding in the square nickel layer implied by Ni−Ni distances of 2.45 Å slightly shorter than those of 2.50 Å in metallic nickel suggests that the actual electron deficiency might not be that large. The dianionic BCB^{2-} ligand just considered can donate an electron pair to the nickel layers both "above" and "below" the BCB ligand, indicating that a *neutral* BCB ligand serves as a net two-electron donor with one electron being donated to each nickel layer. The closed-shell 18-electron nickel configuration for an $Ni(B_2C)_{4/8}^{3-}$ unit can then be obtained as follows:

neutral nickel atom:	10 electrons
the 4 Ni−Ni bonds to the central Ni atom: (4)(1) =	4 electrons
the $(BCB)_{4/8}$ ligand environment: (1/2)(2) =	1 electron
the −3 charge:	3 electrons
Total electronic configuration for each nickel atom in an $Ni(B_2C)_{4/8}^{3-}$ *unit:*	*18 electrons*

The $LnNi_2B_2C$ structure (Figure 3a) can be regarded as a highly anisotropic three-dimensional structure with the two-dimensional Ni layers linked electronically through edge-localized bonding in the unsaturated BCB bridges in the third dimension leading to the layer sequence $(LnC)(Ni_2B_2)$. The nonsuperconducting LuNiBC (Figure 3b) has a similar local environment around each Ni atom but with BC ligands above and below each nickel layer leading to the layer sequence $(LnC)_2Ni_2B_2$. The BC ligands do *not* link adjacent layers in LuNiBC so that LuNiBC has a two-dimensional conducting skeleton, which is delocalized throughout the two dimensions. The differences in the dimensionalities in the conducting skeletons of $LuNi_2B_2C$ and LuNiBC can account for the superconductivity of $LuNi_2B_2C$ but the absence of superconductivity in LuNiBC.[17]

4.3. Ternary Heavy Fermion Superconductors. The relationship between ternary heavy fermion superconductors and other related ternary solid-state structures is summarized in Table 1. An important type of ternary heavy fermion superconductor structure is the $BaAl_4$ structure. The aluminum network in the $BaAl_4$ structure (Figure 4) consists of basal edge-sharing $Al^aAl^b_{4/4}$ square pyramids of aluminum atoms similar to the isolated B_5H_9 square pyramid. The stability of $BaAl_4$ suggests the stability of a polymeric $[Al_4^{2-}]_\infty$ anion containing 14 valence electrons per formula unit.[16] In the heavy fermion superconductor $CeCu_2Si_2$ (T_c = 0.53 K) with a closely related structure,[35] the *neutral* Cu_2Si_2 subnetwork has a total of 10 valence electrons assuming 1 valence electron for each copper atom (i.e., Cu(I) with a filled d^{10} shell) and 4 valence electrons each for each silicon atom. Thus, $Cu_2Si_2^{4-}$ with a Ce^{4+} counterion and Cu(I) in $CeCu_2Si_2$ is isoelectronic with Al_4^{2-} in $BaAl_4$ with a Ba^{2+} counterion because each has 14 valence electrons. Electronic conduction in $CeCu_2Si_2$ can occur through the synchronized valence changes Ce(III)↔Ce(IV) and Cu(I)↔Cu(II) based on the stable oxidation states of cerium and copper. Thus, the 14 valence electrons per $CeCu_2Si_2$ unit can arise from Ce(IV) + 2Cu(I) or Ce(III) + Cu(II) + Cu(I). In the related compounds $EuCu_2Si_2$ and $YbCu_2Si_2$ that are not known to be superconductors, the lanthanide counterions have the oxidation state pairs Ln(II)↔Ln(III) rather than Ln(III)↔Ln(IV) so that the favored 14 valence electrons must arise from Ln(III) + Cu(II) + Cu(I) or Ln(II) + Cu(II). This difference between $EuCu_2Si_2$ and $YbCu_2Si_2$ on one hand and $CeCu_2Si_2$ on the other hand is expected to lead to significant differences in electronic behavior between these two types of materials in accord with experimental observations.

The other ternary heavy fermion superconductor with the $BaAl_4$ structure is URu_2Si_2 (T_c = 1.5 K),[36,37] which may be related to $LaIr_2Si_2$, which is also a superconductor[38] with T_c = 1.6 K. The $Ir_2Si_2^{3-}$ anion in $LaIr_2Si_2$ has 29 valence

Table 1. Some Types of Ternary Heavy Fermion Superconductor Structures

single oxidation state countercations	multiple-oxidation-state countercations	known heavy fermion superconductors
$LaIr_2Si_2$ ($BaAl_4$ structure)	$EuCu_2Si_2$, $YbCu_2Si_2$	$CeCu_2Si_2$, URu_2Si_2
$LuOs_3B_2$	$CeIr_3Si_2$, $CeIr_3B_2$	$CeRu_3B_2$,$CeOs_3B_2$,$CeRu_3Si_2$
Th_2NiC_2	U_2RuC_2, U_2OsC_2, U_2IrC_2, U_2RhC_2	U_2PtC_2

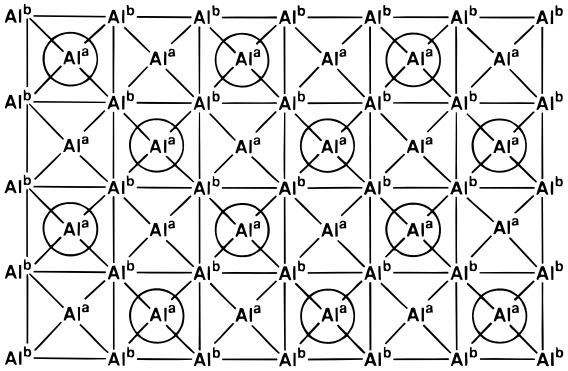

Figure 4. A schematic view of a portion of the aluminum network in $BaAl_4$. Circled aluminum atoms inside the squares appear in front of the page, whereas uncircled aluminum atoms appear in back of the pages. Each $Al^aAl^b_{4/4}$ square corresponds to a square pyramidal cavity.

electrons (including the Ir *d* electrons) and is thus isoelectronic with a 29-valence electron $Ru_2Si_2^{5-}$ implying an average +5 oxidation state for the uranium countercation to attain electroneutrality. This result is consistent with uranium valence fluctuations in the U(IV)↔U(V)↔U(VI) range leading to heavy fermion behavior for URu_2Si_2.

Another type of structure found in heavy fermion superconductors is derived from the $LuOs_3B_2$ structure, which contains boron-centered transition metal trigonal prisms.[39] Each transition metal atom is shared by four such trigonal prisms so that the fundamental structural unit of the anionic network in $LuOs_3B_2$ is the trigonal prismatic cavity $Os_{6/4}B$. The bonding topology within such a centered trigonal prismatic cavity is expected to be edge-localized similar to that in the discrete centered trigonal prismatic $[Co_6(CO)_{15}C]^{2-}$ anion.[40,41] In $LuOs_3B_2$, each of the nine edges of a single $Os_{6/4}B$ trigonal prism is shared between two such trigonal prisms so that a closed-shell electronic configuration for edge-localized bonding has (2)(9/2) = 9 skeletal electrons per trigonal prism corresponding to $Os_{6/4}B^{3-} = Os_3B_2^{6-}$ with each osmium vertex using six internal orbitals and thus serving as a donor of two skeletal electrons.[16] Thus, in $LuOs_3B_2$, each $Os_{6/4}B^{1.5-}$ boron-centered trigonal prism lacks $1^1/_2$ electrons of the closed-shell electronic configuration, leading to holes in its valence band. In $CeRu_3B_2$ and $CeOs_3B_2$, oxidation of Ce(III) to Ce(IV) increases the negative charge on the anionic subnetwork from $M_{6/4}B^{1.5-}$ to $M_{6/4}B^{2-}$, thereby partially filling the holes in the valence band of the anionic network. The corresponding silicides, such as $CeRu_3Si_2$, have an analogous structure with a silicon-centered trigonal prism so that $Ru_{6/4}Si^{2-}$ is isoelectronic with $Os_{6/4}B^{3-}$ is the closed-shell electronic configuration. If the cerium counterion is Ce(IV), then the anionic network in $CeRu_3Si_2$ has this closed shell electronic configuration with a filled valence band. Electron transport in $CeRu_3Si_2$ can occur through reduction of Ce(IV) to Ce(III) concurrently removing an electron from its filled valence band.

The ternary metal carbide U_2PtC_2 is also a heavy fermion superconductor (T_c = 1.5 K). The structure of U_2PtC_2 is analogous to that of Th_2NiC_2, which contains isolated linear $[C-Ni-C]^{8-}$ anions with 26 valence electrons and Ni−C distances of 1.93 Å suggestive of Ni−C single bonding.[42] Assignment of the usual +4 and −4 oxidation states to the Th and isolated carbon atoms, respectively, leads to a formal oxidation state of zero for the nickel atom. The NiC_2^{8-} anion is thus an example of a linear d^{10} metal derivative in which the nickel atom has the favored 14-electron configuration for a two-coordinate linear derivative using a seven-orbital spd^5 bonding manifold.[43] The magnetic susceptibility of U_2PtC_2 corresponds to two unpaired electrons per formula unit[44] suggesting U(IV) analogous to Th(IV) in Th_2NiC_2 and the formulation $U^{IV}{}_2PtC_2$ containing the closed shell PtC_2^{8-} anion isoelectronic with the NiC_2^{8-} anion in Th_2NiC_2. The strong paramagnetism of U_2RuC_2 and U_2OsC_2 exhibiting a weak temperature dependence suggests an intermediate uranium oxidation state and linear diamagnetic RuC_2^{10-} and OsC_2^{10-} anions with a 14-electron configuration similar to that in the isoelectronic NiC_2^{8-} in Th_2NiC_2 already discussed. If U_2RuC_2 and U_2OsC_2 are formulated with the anions RuC_2^{10-} and OsC_2^{10-}, respectively, then the average uranium oxidation state becomes +5. However, the temperature-dependent paramagnetism of U_2RhC_2 and U_2IrC_2 suggests RhC_2^{8-} and IrC_2^{8-} anions with one unpaired electron per transition metal site.[44]

5. SUPERCONDUCTIVITY IN PURE METALS AND BINARY ALLOYS

5.1. Superconductivity and Metal Valence Electrons. Free metals exhibiting T_cs >1 K are generally either early transition metals, such as V, Nb, Ta, Tc, Re, etc., or post-transition metals such as Hg, In, Tl, Sn, and Pb because the magnetism of many middle transition metals such as Mn, Fe, and Co eliminates the possibility of superconductivity. The structures of many of these metals can be constructed by the infinite fusion of metal octahedra in all three dimensions. This process can be modeled stepwise by infinite fusion of metal octahedra first in one dimension to give chains (e.g., Gd_2Cl_3) and then in two dimensions to give sheets (e.g., ZrX) with the limiting case of infinite fusion in all three dimensions corresponding to bulk metals.[16,45] The halogen/metal ratio in such infinite solid-state structures decreases as the number of infinite dimensions (i.e., the "dimensionality") increases (e.g., the halogen/metal ratios are 2 in the "Mo_6Cl_{12}" discrete octahedron, 1.5 in the Gd_2Cl_3 infinite chain structure, 1 in ZrX, and 0 in bulk metals).[45] Atoms shared by two or more such octahedra are partitioned equally between the octahedra in structures generated by the infinite fusion of metal octahedra. Electrons and orbitals from such shared atoms may not necessarily be partitioned equally but the sums of the electrons and the orbitals donated by an atom to all of the units sharing the atom in question must equal the number of valence electrons and orbitals available from the neutral atom, generally three or four electrons and eight or nine orbitals.

The structures of the bulk metals of interest can be considered as infinite arrays of fused octahedra in all three dimensions. In frequently encountered metallic structures, such as the cubic close-packed structures, there are two tetrahedral cavities for each octahedral cavity as in the infinite one-dimensional edge-fused chains of metal octahedra (e.g., Gd_2Cl_3) and infinite edge-fused sheets of metal octahedra (e.g., ZrCl).[45] In a bulk metal, all of the metal valence orbitals are internal orbitals. Because each metal atom is shared by six octahedral cavities and because an octahedral cavity is formed by six metal atoms, the number of valence electrons for each octahedral cavity is equal to the number of valence electrons of the metal. Formation of one multicenter two-electron bond each in each octahedral cavity and in the two tetrahedral cavities for each octahedral cavity requires six electrons per octahedral cavity corresponding to a metal atom with six valence electrons, such as chromium, molybdenum, and tungsten.

This method of treating the chemical bonding topology of bulk metals indicates a special role of the group 6 metals chromium, molybdenum, and tungsten. Such a special role of these metals as forming a "transition metal divide" was recognized by the metallurgist H. E. N. Stone[46] in a study of the systematics of a number of metallic and alloy phases including iron alloys, β-tungsten phases, lanthanide alloys, and Laves phases such as UCo_2 using the "long form" of the periodic table.

(1) The "ionic divide" is familiar to inorganic chemists as the rare gases that separate the elements forming anions (e.g., the halogens) from the elements forming cations (e.g., the alkali metals). The rare gases represent a minimum of chemical reactivity.

(2) The "covalent divide" is located in the C, Si, Ge, Sn, Pb column that separates the compositions of p-type semiconductors with holes as carriers from *n*-type semiconductors with electrons as carriers. The electronic configuration of the elements in the "covalent divide" represent a minimum in conductivity.

(3) The "composite divide" is located at the coinage metals and can be related to the Hume−Rothery approach for the structure of metals and alloys such as brasses.[47]

(4) The "transition metal divide" is located in the Cr, Mo, W column. The electronic configurations of these metals represent a minimum superconducting T_c.

These divides are placed in such positions that any element near to and on one side of a divide will form a compound or compounds with a counterpart element on the opposite side of that divide; if two elements are near to but on the same side of a divide, only less stable compounds or no compounds at all are formed. In the latter case involving only metallic elements, no intermetallic compounds are formed and some other form of phase diagram from solid solubility to liquid insolubility is present.

The requirement of Cooper electron pairs for superconductivity can be related to the graph-theory-derived electronic structure of bulk metals with regard to the effect of the average number of metal valence electrons.[16] This theory indicates a special role for the group 6 metals chromium, molybdenum, and tungsten in forming the so-called "transition metal divide" because their six valence electrons are exactly enough for one multicenter bond for each octahedral cavity and for each of the two tetrahedral cavities associated with each octahedral cavity. This bonding topology corresponds to complete occupancy of these delocalized bonding orbitals with electron pairs (i.e., the analogue of a "closed-shell" electronic configuration) and thus is very unfavorable for the *mobile* Cooper electron pairs required for superconductivity. This result is consistent with the very low T_cs ($<$ 0.1 K) observed for chromium, molybdenum, and tungsten.[48,49]

Now consider the group 5 metals vanadium, niobium, and tantalum, which have much higher T_cs than the group 6 metals just considered. The bonding model just described for the group 5 metals leaves only a single electron rather than an electron pair for one of the three multicenter bonds associated with a given octahedral cavity (including the two tetrahedral cavities associated with each octahedral cavity). These single electrons can interact to form the mobile Cooper pairs required for superconductivity, accounting for the much higher T_cs for group 5 metals relative to the group 6 metals and the local maximum in the T_c versus Z_{av} curve at $Z_{av} = 4.8$ for transition metal alloys, where Z_{av} is the average number of valence electrons per metal atom.[48,49] Similarly, for the group 7 metals technetium and rhenium, the aforementioned bonding model leaves an extra electron after providing electron pairs for each of the three multicenter bonds associated with a given octahedral cavity. Pairing of these extra electrons can lead to the mobile Cooper pairs required for superconductivity, thereby accounting for the much higher T_cs of group 7 metals relative to the group 6 metals and the local maximum in the T_c versus Z_{av} curve at $Z_{av} = 7$ for transition metal alloys. The smaller local maximum in the T_c versus Z_{av} curve at $Z_{av} = 3.3$ may have a similar origin based on pairing of the single electron remaining from each metal atom after an electron pair is provided for each six-center core bond in the centers of the octahedral cavities with no multicenter bonds in the tetrahedral cavities.

A similar relationship between superconductivity and metal valence electrons has also recently been observed in alloys of zirconium with middle-to-late transition metals.[50] Thus, the alloys Zr_2Co and Zr_2Rh with $(4 + 4 + 9)/3 = 5.67$ valence electrons/metal atom have appreciably higher T_cs (i.e., 5.2 and 11.2 K, respectively) than either Zr_2Fe with 5.33 valence electrons/metal atom or Zr_2Ni with 6.0 valence electrons/metal atom. The alloy Zr_2Ni with a T_c of only 2.0 K is isoelectronic with chromium metal, which has a T_c of only 0.08 K.

5.2. Superconductivity in A-15 Alloys. Before the discovery of the high T_c copper oxide superconductors in 1986,[12] the highest T_cs were found in alloys having the so-called A-15 structure and the stoichiometry M_3E in which M is Nb or V and E is Ga, Si, Ge, or Sn.[51,52] Methods analogous to those already described can be used to treat the skeletal bonding topology of the A-15 alloys.

Consider V_3Si as a prototypical A-15 alloy, which may be regarded as isoelectronic with the important A-15 superconductors Nb_3Ge and Nb_3Sn. Figure 5 depicts a cubic building block $V_{12/2}SiSi_{8/8} = V_6Si_2$ of the A-15 structure in which the silicon and vanadium atoms are represented by shaded and open circles, respectively. The structure has the following features:

(1) a silicon atom is in the center of the cube (= Si);

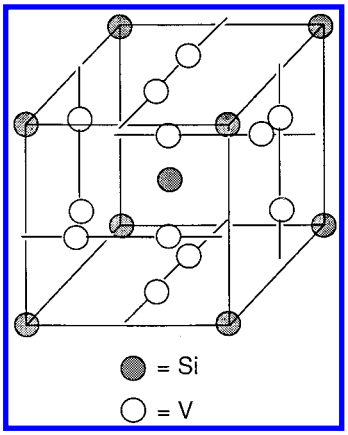

Figure 5. The V_6Si_2 cubic building block for V_3Si and related A-15 superconductors.

(2) silicon atoms are the eight vertexes of the cube, which are each shared with seven other cubes (= $Si_{8/8}$);

(3) pairs of vanadium atoms are in each of the six faces of the cube; each pair is shared with the adjacent cube sharing the same face ($V_{12/2}$); the open circles indicating the pairs of vanadium atoms in a given face are connected by lines for clarity in Figure 5;

(4) the vanadium pairs in the six faces are oriented to form infinite straight vanadium chains in each of the three orthogonal directions; these chains comprise the essential portion of the conducting skeleton;

(5) the polyhedron formed by the 12 vanadium atoms around the central silicon atom is topologically an icosahedron with 20 triangular faces, eight of which are capped by the vertex silicon atoms, thereby forming tetrahedral V_3Si cavities; the $20 - 8 = 12$ uncapped faces of the V_{12} icosahedron occur in six "diamond pairs," in which two adjacent triangular faces have an edge in common.

Consider a chemical bonding topology for V_3Si in which there are two-electron two-center V−V bonds in the infinite straight vanadium chains in the three directions. Six such vanadium chains touch a given V_6Si_2 reference cube (Figure 5); namely, one in each face. The V−V bonds of the vanadium chains, although equivalent in the overall structure, are of the following two types relative to a V_6Si_2 reference cube with which they are associated:

(1) the first type consists of bonds between two vanadium atoms in a given face of the V_6Si_2 reference cube; such V−V bonds are shared only between the two cubes sharing the face containing the vanadium atoms;

(2) the second type consists of bonds between a vanadium atom and the adjacent vanadium atom in the chain *not* associated with the V_6Si_2 reference cube; such V−V bonds are shared between four adjacent V_6Si_2 cubes.

A given V_6Si_2 cube has six V−V bonds of the first type and 12 V−V bonds of the second type. Thus the V−V bonds associated with a given V_6Si_2 reference cube require $(2)(6/2 + 12/4) = 12$ skeletal electrons and use an equivalent number of vanadium valence orbitals because two-electron two-center bonds are being considered.

The chemical bonding topology for V_3Si summarized in Table 2 can now be defined relative to a V_6Si_2 reference cube. Because each vanadium atom uses nine valence orbitals (i.e., an sp^3d^5 valence orbital manifold) and each silicon atom uses four valence orbitals (i.e., an sp^3 valence orbital manifold), the 54 ($= 9 \times 6$) vanadium valence orbitals and eight ($= 2 \times 4$) silicon valence orbitals required for the bonding topology in Table 2 correspond exactly to what is available in a V_6Si_2 cube. A neutral V_6Si_2 cube has $(6)(5) + (2)(4) = 38$ valence electrons, which is two less than the 40 valence electrons required for the chemical bonding topology outlined in Table 2, implying that $V_6Si_2^{2-}$ is the closed-shell electronic configuration for this chemical bonding topology. This model for the chemical bonding in the A-15 superconductors V_3Si and its analogues Nb_3Ge and Nb_3Sn thus has the following features associated with superconductivity as already discussed:

(1) a conducting skeleton in which straight chains of V−V edge-localized bonds are an important component;

(2) holes in the valence band because $V_6Si_2^{2-}$ rather than V_6Si_2 is the closed-shell electronic configuration.

5.3. Heavy Fermion Uranium Alloy Superconductors. Two binary uranium alloys have been found to exhibit heavy fermion superconductivity; namely, UBe_{13} ($T_c = 0.97$ K)[53] and UPt_3 ($T_c = 0.54$ K).[54] In UBe_{13}, the beryllium network consists of $Be^{(1)}Be^{(2)}_{12}$-centered icosahedra packed to form larger 24-atom irregular snub cube cavities of $Be^{(2)}$ atoms surrounding the uranium atoms (Figure 6a).[55] The shortest U···U distances are 5.13 Å, thereby precluding any direct uranium−uranium interaction. Each $Be^{(2)}$ vertex atom of the Be_{12} icosahedra is bonded to four external beryllium vertexes of adjacent icosahedra. Because a neutral beryllium atom has two valence electrons, a *neutral* $Be^{(1)}Be^{(2)}_{12}$ centered icosahedron has exactly the 26 skeletal electrons for delocalized bonding similar to the very stable icosahedral anion $B_{12}H_{12}^{2-}$ if *no* electrons are left for the external bonds to the adjacent $Be^{(1)}Be^{(2)}_{12}$-centered icosahedra. If these external bonds are considered to be five-center $Be^{(2)}_5$ bonds, there is an average of 12/5 such bonds requiring $24/5 = 4.8$ valence electrons for each $Be^{(1)}Be^{(2)}_{12}$-centered icosahedron corresponding to $Be_{13}^{-4.8}$ for a closed-shell electronic configuration leading to an average uranium oxidation state of +4.8. This result is well within the stable uranium oxidation state manifold U(IV)↔U(V)↔U(VI) so that average uranium oxidation states below +4.8 correspond to holes in the valence band of the beryllium network and average uranium oxidation states above +4.8 correspond to electrons in the conduction band of the beryllium network. Thus, in UBe_{13} the uranium valence fluctuations can lead to heavy fermion behavior including heavy fermion superconductivity.

The structure of UPt_3 consists of a lattice of face-centered $U_{8/8}Pt_{6/2}$ cubes (Figure 6b) with the uranium atoms at the vertices and the platinum atoms in the centers of the faces.[56] Each uranium atom is thus shared by eight such cubes whereas each platinum atom is shared by the two cubes sharing the face containing the platinum atom. The $U_{8/8}Pt_{6/2}$ building blocks thus correspond to $Pt_{6/2}$ octahedra within uranium cubes (compare the structural unit of the Chevrel phases in Figure 1). The network of vertex-sharing $Pt_{6/2}$ octahedra separates the uranium atoms in the UPt_3 structure so that the minimum U···U distance is 4.1 Å. Consider these $Pt_{6/2}$ octahedra to be globally delocalized octahedra requiring three internal orbitals from each vertex atom. Then the closed shell configuration for the platinum subnetwork is obtained for $Pt_{6/2}^{2-}$. Because the lowest likely oxidation state for uranium in UPt_3 is +4 corresponding to a $Pt_{6/2}^{4-}$ closed

Table 2. Chemical Bonding Topology of V_3Si and Related A-15 Superconductors Such as Nb_3Ge and Nb_3Sn

bond type	number of such bonds	number of electrons required	number of V orbitals required	number of Si orbitals required
2-center V−V in chains	6	12	12	0
4-center V_3Si in V_3Si tetrahedral cavities	8	16	24	8
3-center V_3 in one V_3 face of each diamond pair	6	12	18	0
Total electrons and orbitals required for one V_6Si_2 cube:		*40*	*54*	*8*

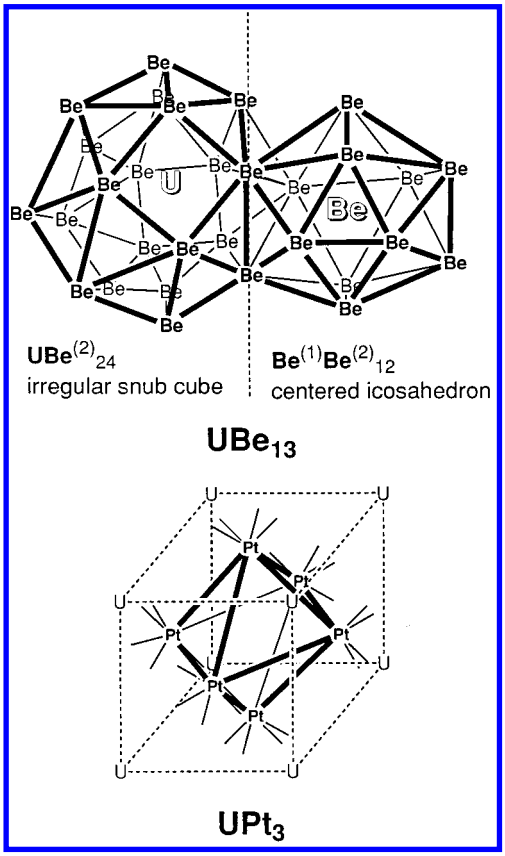

Figure 6. (a) The $Be^{(1)}Be_{12}^{(2)}$ icosahedron and $UBe^{(1)}_{24}$ irregular snub cube building blocks of the UBe_{13} structure showing their linkage. (b) The $U_{8/8}Pt_{6/2}$ building block of the UPt_3 structure showing the $Pt_{6/2}$ octahedron within the $U_{8/8}$ cube.

shell electronic configuration, the compound UPt_3 is electron-rich with electrons in its conduction band. The fact that UPt_3 is electron richer than any other of the heavy fermion superconductors may account for some of its unusual properties compared with other heavy fermion superconductors.[57]

6. OTHER TYPES OF INORGANIC SUPERCONDUCTORS

Some of the ideas just outlined for understanding structure−activity relationships in ternary and quaternary solid-state superconductors are also applicable to other important classes of inorganic superconductors, including the high-temperature copper oxide superconductors as well as reduced fullerene superconductors. Some of the important features of each of these types of superconductors are summarized next.

6.1. Copper Oxide Superconductors. The highest T_c superconductors, namely the copper oxides, do not have direct M−M bonding but instead indirect M−O−M bonding. The well-characterized copper oxide superconductors include the following types, which can be classified by the geometries of their conducting skeletons in which electron transport takes place:

(1) the original 40 K superconductors $La_{2-x}M_xCuO_4$ in which the conducting skeleton consists of a single Cu−O plane;[13,58]

(2) the 90 K "123" superconductor[13,58−60] $YBa_2Cu_3O_7$ and the 81 K "124" superconductor[61] $YBa_2Cu_4O_8$ in which the conducting skeletons consist of two Cu−O planes braced by single or double Cu−O chains, respectively;

(3) the ternary 110 K infinite layer alkaline-earth deficient superconductors[62]

$(Sr_{1-x}Ca_x)_{1-y}CuO_2$;

(4) copper oxide superconductors containing a heavy post-transition element in the row Hg → Bi including the homologous series $HgBa_2Ca_{n-1}Cu_nO_{2n+2}$ (n = 1, 2, 3),[63−66] $Tl_2Ba_2Ca_{n-1}Cu_nO_{2n+4}$ (n = 1, 2, 3),[67] and $Bi_2Sr_2Ca_{n-1}Cu_nO_{2n+4}$ (n = 1, 2, 3),[68,69] as well as the lead derivatives $Pb_2Sr_2LnCu_3O_8$.[70]

The last type of superconductors exhibits the highest T_c values with the maximum reported reliable T_cs being 133, 122, and 115 K for the mercury, thallium, and bismuth derivatives, respectively.

All of the copper oxide superconductors appear to consist of layers of two-dimensional Cu−O conducting skeletons separated by layers of the positive counterions, which can be regarded essentially as insulators. Resistivity[71] and critical magnetic field[72] measurements provide evidence for the two-dimensional nature of the conducting skeletons in these materials. Increasing the rigidity of the two-dimensional conducting skeleton by coupling the Cu−O layers either by bracing with a Cu−O chain in $YBa_2Cu_3O_{7-y}$ or by close proximity in the higher members of the homologous series $M^{III}{}_2M^{II}{}_2Ca_{n-1}Cu_nO_{2n+4}$ (M^{III} = Tl, M^{II} = Ba, or M^{III} = Bi, M^{II} = Sr) leads to increases in T_c. The presence of mercury, thallium or bismuth layers appears to lead to somewhat higher T_cs. This observation coupled with computations of the electronic band structure of $Bi_2Sr_2CaCu_2O_8$[73,74] and the low resistivity of Tl_2O_3 suggests that electron transport may occur in the Bi−O or Tl−O layers as well as the Cu−O layers in the $M^{III}{}_2M^{II}{}_2Ca_{n-1}Cu_nO_{2n+4}$ materials. Destruction of the two-dimensional structure of copper oxide derivatives by gaps in the Cu−O planes or by Cu−O chains in the third dimension leads to mixed copper oxides that are metallic but not superconducting,[75] such as $La_2SrCu_2O_6$, $La_4BaCu_5O_{13}$, and $La_5SrCu_6O_{15}$.

The two-dimensional conducting skeletons in these copper oxide superconductors are constructed from networks of Cu−O edge-localized bonds and analogous to the localized metal−metal bonding in the Chevrel phases,[9] lanthanide rhodium borides,[10] A-15 alloys,[16] and other superconductors with direct M−M rather than indirect M−O−M bonding. The following points are of interest concerning the chemical bonding topology of the copper oxide superconductors:

(1) the conducting skeleton is constructed from Cu−O−Cu bonds rather than direct Cu−Cu bonds; the much higher ionic character and thus much lower polarizability and higher rigidity of metal−oxygen bonds relative to metal−metal bonds can be related to the persistence of superconductivity in copper oxides to much higher temperatures than that in metal clusters;

(2) the required metal−metal interactions are antiferromagnetic interactions between the single unpaired electrons in the d_{xy} orbitals of two d^9 Cu(II) ions separated by an oxygen bridge similar to antiferromagnetic Cu(II)−Cu(II) interactions in discrete binuclear complexes.[76,77] This general idea has been presented by Anderson and co-workers as the so-called resonating valence bond model.[78,79]

(3) the positive counterions in the copper oxide superconductors control the negative charge on the Cu−O skeleton and hence the oxidation states of the copper atoms; positive counterions, which are "hard" in the Pearson sense[80] in preferring to bind to nonpolarizable bases, such as the lanthanides and alkaline earths, do not contribute to the conductivity; however, layers of the positive counterions mercury, thallium, or bismuth, which are "soft" in the Pearson sense in preferring to bind to polarizable bases, may contribute to the conductivity as already noted;

(4) partial oxidation of some of the Cu(II) to Cu(III) in the copper oxide superconductors just listed generates holes in the conduction band required for conductivity; this is in accord with Hall effect measurements[81] that show positive Hall coefficients, indicating that holes rather than electrons are the current carriers; in addition, 28 K superconductors with the general formula $Ln_{2-x}Ce_xCuO_4$ (Ln = Pr, Nd, Sm) are known,[82,83] which have negative Hall coefficients, indicating that mobile electrons are the current carriers; these mobile electrons arise by partial reduction of some of the Cu(II) to Cu(I).

6.2. Superconductivity in Fullerenes. The superconducting phases derived from the C_{60} fullerene structure have the stoichiometries A_3C_{60} (A = alkali metal)[84] and exhibit T_cs around 20 K (e.g., 18 K for K_3C_{60}). These superconducting materials retain the solid-state C_{60} face-centered cubic structure with slightly modified lattice constants and thus may be regarded as three-dimensional materials. More extensive reduction of C_{60} with alkali metals leads to insulating orthorhombic A_4C_{60} and insulating body-centered cubic A_6C_{60} phases.

The origin of the superconductivity in these reduced C_{60} materials can be understood by consideration of the electronic structure of C_{60}.[85] The bonding character in the C_{60} cage may be regarded as predominantly sp^2 with a small amount of sp^3 character arising from the nonzero curvature of the C_{60} surface. The bonding σ-states (i.e., the valence band) of C_{60} relate to edge-localized σ-bonds along the 90 edges of the truncated icosahedron and reside well below the highest occupied molecular orbital (HOMO) of C_{60}, which is composed of orbitals having primarily π character.

The following additional points can relate to the superconducting properties of C_{60}^{3-} salts of relatively compact cations such as K^+:

(1) electronic communication between adjacent C_{60}^{3-} cages is necessary to allow the transfer of electrons and/or holes in the incompletely filled HOMO of C_{60}^{3-} required for electrical conductivity. The countercations in superconducting C_{60}^{3-} salts must be small enough to allow some overlap of the π-orbitals in adjacent C_{60} cages for this electronic communication;

(2) the large size of the C_{60} truncated icosahedron restricts the delocalization of its 60 p electrons to the surface of the polyhedron in contrast to deltahedral boranes such as the anions $B_nH_n^{2-}$ ($6 = n = 12$) in which core bonding in the center of the deltahedron is an important aspect of the delocalization in such boranes. Thus in C_{60} the π-electron density in the center of the truncated icosahedron may be regarded as negligible so that the π-electron network in C_{60} structures corresponding to the conducting skeleton in C_{60}^{3-}-containing materials is porous. This idea links the concept of porous delocalization already developed for metal cluster superconductors to the superconductivity found in K_3C_{60} and related C_{60}^{3-} materials.

7. SUMMARY

Electrical conductivity is well-known to require a structure containing mobile electrons that can arise from holes in an otherwise filled valence band (*p*-type conductors) or electrons in an otherwise empty conduction band (*n*-type conductors). Superconductivity is favored when this electron mobility is restricted to fewer than three dimensions typically by constructing the conducting skeleton through edge-localized rather than more extensively delocalized bonding. Thus the chemical bonding topologies of the highest T_c superconductors contain one of the following features:

(1) edge-localized M−M bonding in the conducting skeletons of ternary and quaternary solid-state superconductors or related partially localized bonding in superconducting transition metals and their alloys;

(2) edge-localized Cu−O bonding in copper oxide superconductors containing Cu−O−Cu linkages with appreciable Cu···Cu antiferromagnetic interactions;

(3) surface-localized bonding in fullerene superconductors containing direct C−C bonds.

In addition, heavy fermion superconductors having considerably lower T_cs are known in which the conducting skeleton consists of variable oxidation state lanthanide or actinide cations diluted by an anionic network of other metal atoms.

REFERENCES AND NOTES

(1) Rouvray, D. H. The Modeling of Chemical Phenomena Using Topological Indices. *J. Comput. Chem.* **1987**, *8*, 470.
(2) Trinajstić, N. *Chemical Graph Theory*, 2nd ed; CRC: Boca Raton, FL, 1992; Chapter 10.
(3) King, R. B. Mathematical Inorganic Chemistry: From Gas-Phase Metal Clusters to Superconducting Solids. *Acc. Chem. Res.* **1992**, *25*, 247.
(4) King, R. B. *Applications of Graph Theory and Topology in Inorganic Cluster and Coordination Chemistry*; CRC: Boca Raton, FL, 1993; 229 pp.
(5) Buckel, W. *Superconductivity: Fundamentals and Applications*; VCH: New York, 1991.
(6) Cyrot, M.; Pavuna, D. *Introduction to Superconductivity and High-T_c Materials*; World Scientific: Singapore, 1992.
(7) Poole, C. P., Jr.; Farach, H. A.; Creswick, R. J. *Superconductivity*; Academic: San Diego, 1995.
(8) Tinkham, M. *Introduction to Superconductivity*; McGraw-Hill: New York, 1996.
(9) King, R. B. Chemical Bonding Topology of Superconductors. 1. Ternary Molybdenum Chalcogenides (Chevrel Phases). *J. Solid State Chem.* **1987**, *71*, 224.

(10) King, R. B. Chemical Bonding Topology of Superconductors. 2. Ternary Lanthanide Rhodium Borides. *J. Solid State Chem.* **1987**, *71*, 233.
(11) Bardeen, J.; Cooper, L. N.; Schrieffer, J. R. *Phys. Rev.* **1957**, *108*, 1175.
(12) Bednorz, J. G.; Müller, K. A. Possible High T_c Superconductivity in the Ba−La−Cu−O System. *Z. Phys. B* **1986**, *64*, 189.
(13) Williams, J. M.; Beno, M. A.; Carlson, K. D.; Geiser, U.; Ivy Kao, H. C.; Kini, A. M.; Porter, L. C.; Schultz, A. J.; Thorn, R. J.; Wang, H. H.; Whangbo, M.-H.; Evain, M. High Transition Temperature Inorganic Oxide Superconductors: Synthesis, Crystal Structure, Electrical Properties, and Electronic Structure. *Acc. Chem. Res.* **1988**, *21*, 1.
(14) Poole, C. P., Jr.; Datta, T.; Farach, H. A. *Copper Oxide Superconductors*; Wiley: New York, 1988.
(15) King, R. B. The Relationship of the Chemical Bonding Topology of High Critical Temperature Copper Oxide Superconductors to that of the Chevrel Phases and the Ternary Lanthanide Rhodium Borides. *Inorg. Chim. Acta* **1988**, *143*, 15.
(16) King, R. B. Topological Aspects of the Chemical Bonding in Superconducting Transition Metal Borides, Silicides, and Alloys. *Inorg. Chem.* **1990**, *29*, 2164.
(17) King, R. B. Chemical Bonding Topology of Superconductors. 3. Layered Quaternary Lanthanide Nickel Borocarbides and Boronitrides. *J. Solid State Chem.* **1996**, *124*, 329.
(18) King, R. B. Chemical Bonding Topology of Superconductors. 4. Heavy Fermion Superconductors. *J. Solid State Chem.* **1997**, *131*, 394.
(19) King, R. B. The Concept of Porous Delocalization in Superconductors. In *Concepts in Chemistry*; Rouvray, D. H.; Kirby, E., Eds.; Research Studies Press: Taunton, England, 1996; pp 235−263.
(20) Grünbaum, B. *Convex Polytopes*; Interscience: New York, 1967.
(21) Stewart, G. R. Heavy Fermion Systems. *Rev. Mod. Phys.* **1984**, *56*, 755.
(22) Schäfer, H.; Schnering, H.; Tillack, J.; Kuhnen, F.; Wöhler, H.; Baumann, H. Neue Untersuchungen über die Chloride des Molybdäns. *Z. anorg. allgem. Chem.* **1967**, *353*, 281.
(23) Fischer, Ø. Chevrel Phases: Superconducting and Normal State Properties. *Appl. Phys.* **1978**, *16*, 1.
(24) Chevrel, R.; Gougeon, P.; Potel, M.; Sergent, M. Ternary Molybdenum Chalcogenides: A Route to New Extended Clusters. *J. Solid State Chem.* **1985**, *57*, 25.
(25) Matthias, B. T.; Marezio, M.; Corenzwit, E.; Cooper, A. S.; Barz, H. E. High-Temperature Superconductors. The First Ternary System. *Science* **1972**, *175*, 1465.
(26) Burdett, J. K.; Lin, J.-H. Structure of Chevrel Phases. *Inorg. Chem.* **1982**, *21*, 5.
(27) Fischer, Ø.; Decroux, M.; Chevrel, R.; Sergent, M. On the Upper Critical Field of the Ternary Molybdenum Chalcogenides. In *Superconductivity in* d- *and* f-*Band Metals*, Douglas, D. H., Ed.; Plenum: New York, 1976; pp 176−177.
(28) Matthias, B. T.; Corenzwit, E.; Vandenberg, J. M.; Barz, H. E. High Superconducting Transition Temperatures of New Rare Earth Ternary Borides. *Proc. Natl. Acad. Sci. U.S.A.* **1977**, *74*, 1334.
(29) Woolf, L. D.; Johnston, D. C.; MacKay, H. B.; McCallum, R. W.; Maple, M. B. Superconducting and Normal State Properties of $ErRh_4B_4$ and $LuRh_4B_4$. *J. Low Temp. Phys.* **1979**, *35*, 651.
(30) Vandenberg, J. M.; Matthias, B. T. Crystallography of New Ternary Borides. *Proc. Natl. Acad. Sci. U.S.A.* **1977**, *74*, 1336.
(31) Carré, F. H.; Cotton, F. A.; Frenz, B. A. Preparation and Structure of a New Derivative of Tetrarhodium Dodecacarbonyl. Further Refinement of the Structure of Tetracobalt Dodecacarbonyl. *Inorg. Chem.* **1976**, *15*, 380.
(32) Sheldon, R. N.; Karcher, B. A.; Powell, D. R.; Jacobson, R. A.; Ku, H. C. Crystal Structure of $LuRuB_2$. *Mater. Res. Bull.* **1980**, *15*, 1445.
(33) Halet, J. F. Electronic Structure of the Superconducting Rare-Earth-Metal Nickel Boron Carbide Compounds. *Inorg. Chem.* **1994**, *33*, 4173.
(34) Cava, R. J.; Takagi, H.; Zandbergen, H. W.; Krajewski, J. J.; Peck, W. F. Jr.; Siegrist, T.; Batlogg, B.; van Dover: R. B.; Felder, R. J.; Mizuhashi, K.; Lee, J. O.; Eisaki, H.; Uchida, S. Superconductivity in the Quaternary Intermetallic Compounds $LnNi_2B_2C$. *Nature* **1994**, *367*, 252.
(35) Rossi, D.; Marazza, R.; Ferro, R. Ternary RMe_2X_2 Alloys of the Rare Earths with the Precious Metals and Silicon (or Germanium). *J. Less-Common Met.* **1979**, *66*, 17.
(36) Dalichaouch, Y.; Maple, M. B.; Chen, J. W.; Kohara, G.; Rossel, C.; Torikachvili, M. S.; Giorgi, A. L. Effect of Transition Metal Substitutions on Competing Electronic Transitions in the Heavy-electron Compound URu_2Si_2. *Phys. Rev.* **1990**, *41*, 1829.
(37) Boholm, C.; Kjems, J. K.; Buyers, W. J. L.; Matthew, P.; Palstra, T. T. M.; Menovsky, A. A.; Mydosh, J. A. U_2PtC_2 and Systematics of Heavy Fermions. *Phys. Rev. Lett.* **1987**, *53*, 1829.
(38) Braun, H. F. Superconductivity in Ternary Rare Earth-Transition Metal Silicides: A Critical Review. *J. Less-Common Met.* **1984**, *100*, 105.
(39) Niihara, K.; Yajima, S. The Preparation and Crystal Structure of Ternary Rare Earth Borides. *Bull. Chem. Soc. Jpn.* **1973**, *46*, 770.
(40) Martinengo, S.; Strumolo, D.; Chinik, P.; Albano, V. G.; Braga, D. New Carbide Clusters in the Cobalt Subgroup. Part 13. Synthesis and Chemical Characterization of the Anions $[Co_6C(CO)_{14}]^-$, $[Co_6C(CO)_{15}]^{2-}$, and $[Co_8C(CO)_{18}]^{2-}$, and Crystal Structure of μ_6−Carbido-ennea-μ-carbonyl-hexacarbonyl-*polyhedro*-hexacobaltate(2−) as its Benzyltrimethylammonium Salt; a Comparison with Isostructural Species. *J. Chem. Soc., Dalton* **1985**, 35.
(41) King, R. B. Metal Cluster Topology. 6. Cobalt Carbonyl Clusters Containing Interstitial Carbon Atoms. *New J. Chem.* **1988**, *12*, 493.
(42) Moss, M. A.; Jeitschko, W. Kristallstrukturen und Eigenschaften der Thorium−Nickel-Carbide $Th_3Ni_5C_5$ and Th_2NiC_2. *Z. anorg. allgem. Chem.* **1991**, *603*, 57.
(43) King, R. B. The Role of Toroidal and Cylindrical Chemical Bonding Manifolds in Coinage Metal and Mercury Clusters. *J. Chem. Inf. Comput. Sci.* **1994**, *34*, 410.
(44) Ebel, T.; Wachtmann, K. H.; Jeitschko, W. Magnetic Properties of the Uranium Transition Metal Carbides U_2TC_2 (T = Ru, Os, Rh, Ir, and Pt). *Solid State Comm.* **1996**, *97*, 815.
(45) King, R. B. Metal Cluster Topology. 5. Infinite Delocalization in One and Two Dimensions: Lanthanide and Early Transition Metal Halide Clusters Built from Fused Octahedra. *Inorg. Chim. Acta* **1987**, *129*, 91.
(46) Stone, H. E. N. Alloy Systematics in Relation to the Long Periodic Table. *Acta Metallurgica* **1979**, *27*, 259.
(47) Hume−Rothery, W.; Smallman, R. E.; Haworth, C. W. *The Structure of Metals and Alloys*; The Metals and Metallurgy Trust: London, 1969.
(48) Matthias, B. T. *Phys. Rev.* **1955**, *97*, 74.
(49) Matthias, B. T. In *Progress in Low-Temperature Physics II*; Gorter, C. J., Ed.; North-Holland: Amsterdam, 1975: Chapter 5, pp 138−150.
(50) Salunke, H. G.; Das, G. P.; Raj, P.; Sahni, V. C.; Dhar, S. K. Band Filling and Superconductivity in Zr_2M Compounds. *Physica C* **1994**, *226*, 385.
(51) Leger, J. M. Search for Superconductors above 20 K. *J. Low Temp. Phys.* **1974**, *14*, 297.
(52) Johnson, G. R.; Douglass, D. H. Superconductivity in New A-15 Niobium Alloys. *J. Low Temp. Phys.* **1974**, *14*, 575.
(53) Ott, H. R.; Rudigier H.; Fisk, Z.; Smith, J. L. UBe_{13}: An Unconventional Actinide Superconductor. *Phys. Rev. Lett.* **1983**, *50*, 1595.
(54) Stewart, G. R.; Fisk, Z.; Willis, J. O.; Smith, J. L. Possibility of Coexistence of Bulk Superconductivity and Spin Fluctuations in UPt_3. *Phys. Rev. Lett.* **1984**, *52*, 679.
(55) McElfrish, M. W.; Hall, J. H.; Ryan, R. R.; Smith, J. L.; Fisk, Z. Structure of the Heavy-Fermion Superconductor UBe_{13}. *Acta Crystallogr.* **1990**, *C46*, 1579.
(56) Heal, T. J.; Williams, G. I. Compounds of Uranium with the Transition Metals of the Second and Third Long Periods. *Acta Crystallogr.* **1955**, *8*, 494.
(57) Stewart, G. R. Spin Fluctuations and Superconductivity in UPt_3. *J. Appl. Phys.* **1985**, *57*, 3049.
(58) Wang, H. H.; Geiser, U.; Thorn, R. J.; Carlson, K. D.; Beno, M. A.; Monaghan, M. R.; Allen, T. J.; Prokasch, R. B.; Stupka, D. L.; Kwok, W. K.; Crabtree, G. W.; Williams, J. M. Synthesis, Structure, and Superconductivity of Single Crystals of High-T_c $La_{1.85}Sr_{0.15}CuO_4$. *Inorg. Chem.* **1987**, *26*, 1190.
(59) Wu, M. K.; Ashburn, J. R.; Torng, C. J.; Hor, P. H.; Meng, R. L.; Gao, L.; Huang, Z. L.; Wang, Y. Q.; Chu, C. W. Superconductivity at 93 K in a New Mixed-Phase Y−Ba−Cu−O Compound System at Ambient Pressure. *Phys. Rev. Lett.* **1987**, *58*, 908.
(60) Whangbo, M. H.; Evain, M.; Beno, M. A.; Williams, J. M. Band Electronic Structure of the High-Temperature (T_c > 90 K) Superconductor Orthorhombic $YBa_2Cu_3O_7$. 1. Partially Filled *d*-Block Bands of the Equilibrium Structure. *Inorg. Chem.* **1987**, *26*, 1831.
(61) Karpinski, J.; Kaldis, E.; Jilek, E.; Rusiocik, S.; Bucher, B. Bulk Synthesis of the 81-K Superconductor $YBa_2Cu_4O_8$ at High Oxygen Pressures. *Nature* **1988**, *336*, 660.
(62) Azuma, M.; Hirori, Z.; Takano, M.; Baudo, Y.; Takeda, Y. Superconductivity at 110 K in the Infinite-Layer Compound $(Sr_{1-x}Ca_x)_{1-y}CuO_2$. *Nature* **1992**, *356*, 775.
(63) Huang, Z. L.; Meng, R. L.; Qiu, X. D.; Sun, Y. Y.; Kulik, J.; Xue, Y. Y.; Chu, C. W. Superconductivity, Structure, and Resistivity in $HgBa_2Ca_2Cu_3O_{8+\delta}$. *Physica C* **1993**, *217*, 1.
(64) Putlin, S. N.; Antipov, E. V.; Chmaissem, O.; Marezio, M. Superconductivity at 94 K in $HgBa_2CuO_{4+\delta}$. *Nature* **1993**, *362*, 226.
(65) Rodriguez, C. O.; Christense, N. E.; Peltzer y Blancá, E. L. Electronic Structure of Mercury-based High T_c Compounds $HgBa_2Ca_{n-1}Cu_nO_{2n+2}$. *Physica C* **1993**, *216*, 12.

(66) Loureiro, S. M.; Antipov, E. V.; Tholence, J. L.; Caponi, J. J.; Chmaissem, O.; Huang, Q.; Marezio, M. Synthesis and Structural Characterization of the 127 K $HgBa_2CaCu_2O_{6.22}$ Superconductor. *Physica C* **1993**, *217*, 253.
(67) Hazen, R. M.; Finger, L. W.; Angel, R. J.; Prewitt, C. T.; Ross, N. L.; Hadidacos, C. G.; Heaney, P. J.; Veblen, D. R.; Sheng, Z. Z.; El Ali, A.; Hermann, A. M. 100-K Superconducting Phases in the Tl−Co−Ba−Cu−O System. *Phys. Rev. Lett.* **1988**, *60*, 1657.
(68) Hazen, R. M.; Prewitt, C. T.; Angel, R. J.; Ross, N. L.; Finger, L. W.; Hadidacos, C. G.; Veblen, D. R.; Heaney, P. J.; Hor, P. H.; Meng, R. L.; Sun, Y. Y.; Wang, Y. Q.; Xue, Y. Y.; Huang, Z. J.; Gao, L.; Bechtold, J.; Chu, C. W. Superconductivity in the High-T_c Bi−Ca−Sr−Cu−O System: Phase Identification. *Phys. Rev. Lett.* **1988**, *60*, 1174.
(69) Subramanian, M. A.; Torardi, C. C.; Calabrese, J. C.; Gopalakrishnan, J.; Morrissey, K. J.; Askew, T. R.; Flippen, R. B.; Chowdhry, U.; Sleight, A. W. A New High-Temperature Superconductor: $Bi_2Sr_{3-x}Ca_x$-Cu_2O_{8+y}. *Science* **1988**, *239*, 1015.
(70) Cava, R. J.; Batlogg, B.; Krajewski, J. J.; Rupp, L. W.; Schneemeyer, L. F.; Siegrist, T.; van Dover: R. B.; Marsh, P.; Peck, W. F., Jr.; Gallagher, P. K.; Glarum, S. H.; Marshall, J. H.; Farrow, R. C.; Waszczak, J. W.; Hull, R.; Trevor, P. Superconductivity near 70 K in a New Family of Layered Copper Oxides. *Nature* **1988**, *336*, 211.
(71) Cheong, S. W.; Fisk, Z.; Kwok, R. S.; Remeika, J. P.; Thomson, J. D.; Gruner, C. Electronic Anisotropy in Single-Crystal La_2CuO_4. *Phys. Rev. B* **1988**, *37*, 5916, 1988.
(72) Moodera, J. S.; Meservey, R.; Tkaczyk, J. E.; Hao, C. X.; Gibson, G. A.; Tedrow, P. M. Critical-Magnetic-Field Anisotropy in Single-Crystal $YBa_2Cu_3O_7$. *Phys. Rev. B* **1988**, *37*, 619.
(73) Hybertsen M. S.; Mattheiss, L. F. Electronic Band Structure of $CaBi_2$-$Sr_2Cu_2O_8$. *Phys. Rev. Lett.* **1988**, *60*, 1661.
(74) Krakauer, H.; Pickett, W. E. Effect of Bismuth on High-T_c Cuprate Superconductors. *Phys. Rev. Lett.* **1988**, *160*, 1665.
(75) Torrance, J. B.; Tokura, Y.; Nazzal, A.; Parkin, S. S. P. Metallic, but not Superconducting, La−Ba (and La−Sr) Copper Oxides. *Phys. Rev. Lett.* **1988**, *60*, 542.
(76) Doedens, R. J. Structure and Metal−Metal Interactions in Copper(II) Carboxylate Complexes. *Progr. Inorg. Chem.* **1976**, *21*, 209.
(77) Cairns C. J.; Busch, D. H. Intramolecular Ferromagnetic Interactions in Polynuclear Metal Complexes. *Coord. Chem. Rev.* **1986**, *69*, 1.
(78) Anderson, P. W. The Resonating Valence Bond State in La_2CuO_4 and Superconductivity. *Science* **1987**, *235*, 1196.
(79) Anderson, P. W.; Baskaran, G.; Zou, Z.; Hsu, T. Resonating Valence Bond Theory of Phase Transitions and Superconductivity in La_2CuO_4−Based Compounds. *Phys. Rev. Lett.* **1987**, *58*, 2790.
(80) Pearson, R. G. Hard and Soft Acids and Bases. *J. Am. Chem. Soc.* **1963**, *85*, 3533.
(81) Ong, N. P.; Wang, Z. Z.; Clayhold, J.; Tarascon, J. M.; Greene, L. H.; McKinnon, W. R. Hall Effect of $La_{2-x}Sr_xCuO_4$: Implications for the Electronic Structure in the Normal State. *Phys. Rev. B* **1987**, *35*, 8807.
(82) Tokura, Y.; Takagi, H.; Uchida, S. A Superconducting Copper Oxide Compounds with Electrons as the Charge Carriers. *Nature* **1989**, *337*, 345.
(83) Sawa, H.; Suzuki, S.; Watanabe, M.; Akimitsu, J.; Matsubara, H.; Watabe, H.; Uchida, S.; Kokusho, K.; Asano, H.; Izumi, F.; Takayama-Muromachi, E. Unusually Simple Crystal Structure of an Nd−Ce−Sr−Cu−O Superconductor. *Nature* **1989**, *337*, 347.
(84) Stephens, P. W.; Mihaly, L.; Lee, P. L.; Whetten, R. L.; Huang, S.-M.; Kaner, R. F.; Diederich, F.; Holczer, K. Structure of Single-Phase Superconducting K_3C_{60}. *Nature* **1991**, *351*, 632.
(85) Elser, V.; Haddon, R. C. Icosahedral C_{60}: an Aromatic Molecule with a Vanishingly Small Ring Current Magnetic Susceptibility. *Nature* **1987**, *325*, 792.

CI980050B